

Strain-manipulated dispersion characteristics of magnonic crystals with Dzyaloshinskii-Moriya interaction and applications on spin-wave devices

Chuhan Zhou(周楚涵), Xiaotian Jiao(焦晓天), Jiaxi Xu(徐佳熙), Zhaonian Jin(金兆年), Lin Chen(陈琳), and Zhikuo Tao(陶志阔)

Citation: Chin. Phys. B, 2025, 34 (**2**): 027501. DOI: 10.1088/1674-1056/ad9892
Journal homepage: http://cpb.iphy.ac.cn; http://iopscience.iop.org/cpb

What follows is a list of articles you may be interested in

Skyrmion motion induced by spin-waves on magnetic nanotubes

Tijjani Abdulrazak, Xuejuan Liu(刘雪娟), Zhenyu Wang(王振宇), Yunshan Cao(曹云姗), and Peng Yan(严鹏)
Chin. Phys. B, 2024, 33 (**10**): 107504. DOI: 10.1088/1674-1056/ad5d64

Consistency between domain wall oscillation modes and spin wave modes in nanostrips

Xinwei Dong(董新伟) and Zhenjiang Wu(吴振江)
Chin. Phys. B, 2024, 33 (**6**): 067502. DOI: 10.1088/1674-1056/ad2a6b

Tunable dispersion relations manipulated by strain in skyrmion-based magnonic crystals

Zhao-Nian Jin(金兆年), Xuan-Lin He(何宣霖), Chao Yu(于超), Henan Fang(方贺男), Lin Chen(陈琳), and Zhi-Kuo Tao(陶志阔)
Chin. Phys. B, 2024, 33 (**1**): 017501. DOI: 10.1088/1674-1056/acf03c

Magnonic band-pass and band-stop filters with structurally modulated waveguides

Lai-He Feng(冯来和), Mang-Yuan Ma(马莽原), Zhi-Hua Liu(刘智华), Kai-Le Xie(解凯乐), and Fu-Sheng Ma(马付胜)
Chin. Phys. B, 2023, 32 (**6**): 067503. DOI: 10.1088/1674-1056/ac8afb

Effects of rotating noncircular scatterers on spin-wave band gaps of two-dimensional magnonic crystals

Yang Hui (杨慧), Yun Guo-Hong (云国宏), Cao Yong-Jun (曹永军)
Chin. Phys. B, 2014, 23 (**9**): 097501. DOI: 10.1088/1674-1056/23/9/097501

Strain-manipulated dispersion characteristics of magnonic crystals with Dzyaloshinskii–Moriya interaction and applications on spin-wave devices

Chuhan Zhou(周楚涵)[1], Xiaotian Jiao(焦晓天)[2], Jiaxi Xu(徐佳熙)[1], Zhaonian Jin(金兆年)[1], Lin Chen(陈琳)[2], and Zhikuo Tao(陶志阔)[2,†]

[1] *Bell Honors School, Nanjing University of Posts and Telecommunications, Nanjing* 210003, *China*
[2] *College of Electronic and Optical Engineering & College of Flexible Electronics, Nanjing University of Posts and Telecommunications, Nanjing* 210003, *China*

(Received 25 July 2024; revised manuscript received 26 November 2024; accepted manuscript online 29 November 2024)

Dispersion characteristics of magnonic crystals have attracted considerable attention because of the potential applications for spin-wave devices. In this work, we investigated the strain-manipulated dispersion characteristics of magnonic crystals with Dzyaloshinskii–Moriya interaction (DMI) and discussed the potential applications in spin-wave devices. Here, the ground states and stabilities of the magnonic crystals were investigated. Then, the strain-manipulated dispersion characteristics of the magnonic crystals based on domains and skyrmions were studied. The simulation results indicated that, the applied strain could manipulate the band widths and the positions of the allowed frequency bands. Finally, the realization of magnonic crystal heterojunctions and potential applications in spin-wave devices, such as filters, diodes, and transistors based on strain-manipulated magnonic crystals were proposed. Our research provides a theoretical foundation for designing tunable spin-wave devices based on strain-manipulated magnonic crystals with DMI.

Keywords: magnonic crystal, spin wave, dispersion relation, skyrmion, domain

PACS: 75.30.Ds, 75.80.+q, 85.70.Ay, 12.39.Dc

DOI: 10.1088/1674-1056/ad9892 **CSTR:** 32038.14.CPB.ad9892

1. Introduction

Spin waves can propagate in magnetically ordered materials and cannot dissipate Joule heating which is an obstacle in the semiconductor-based electronics.[1] As the quanta of the magnetic excitations, spin waves are also known as magnons, which can be used to carry digital information in magnonics.[2] Similar to semiconductor crystals and photonic crystals, periodically modulated magnetic structures in magnonic crystals (MCs) can exhibit dispersion characteristics (frequency f versus wave-vector k) which present allowed magnonic frequency bands and prohibited magnonic bandgaps.[3,4]

As topologically stable spin configurations, domains and skyrmions are usually arranged periodically to form magnonic crystals.[5–9] Basically, the spin configurations of skyrmion and other topological magnetic textures, such as skyrmionium, meron, and hopfion which can be used as the blocks of magnonic crystals, are determined by chiral Dzyaloshinskii–Moriya interaction (DMI).[10,11] DMI is an antisymmetric interaction induced by spin–orbit coupling, which exists widely in non-centrosymmetric magnetic bulk compounds and thin layers with the breaking of inversion symmetry. Kinds of topologically magnetic textures can be formed through competitions between DMI and Heisenberg exchange interactions, together with anisotropy and other contributing energies. Moreover, interactions between spin waves and magnetic textures were investigated, such as the motion of magnetic textures driven by spin waves,[12–18] and the tailor of spin-wave dispersion relations by manipulating the magnetic textures.[19–21]

The dispersion characteristics of magnonic crystals can be tailored by the geometry design, parameter evaluation, and especially the manipulation of extent applied methods such as electric fields, magnetic fields, and strains.[5,9] For example, the skyrmion-based magnonic crystals can be generated and annihilated by spin-polarized current pulses[5] or external magnetic field.[9] Recently, magneto-elastic coupling or strain effect has provided a new method to manipulate the topological spin configurations, such as generation, annihilation or tuning.[22–29] Considering that, the strain can be induced by applied electric field through converse piezoelectric effect, voltage-manipulation can be a convenient and effective method to design and tailor the band structures or dispersion relations of magnonic crystals with DMI.

In this work, we theoretically investigated the strain-manipulated dispersion characteristics of magnonic crystals with DMI and proposed the potential applications in spin-wave devices. Firstly, we investigated the ground states of the magnonic crystals. Secondly, we studied the strain-

†Corresponding author. E-mail: zktao@njupt.edu.cn

© 2025 Chinese Physical Society and IOP Publishing Ltd. All rights, including for text and data mining, AI training, and similar technologies, are reserved.

manipulated dispersion characteristics of the magnonic crystals based on domains and skyrmions. Finally, we proposed the potential applications in spin-wave devices such as filters, diodes and transistors based on strain-manipulated magnonic crystals.

2. Simulation methods

The strain-manipulated dispersion relations of the magnonic crystals were simulated by Object Oriented Micro-Magnetic Framework (OOMMF)[30] embedded in Ubermag which provides a unified interface to solve micromagnetic problems.[31]

Firstly, we investigated the ground states of the magnonic crystals by calculating the minimum value of the total energy $E_{\rm tot}$. We started with a two-dimensional (2D) Heisenberg model with the nearest neighbor ferromagnetic exchange, uniaxial anisotropy along the z-axis, Zeeman field, interfacial DMI, and strain-manipulated magneto-elastic coupling. The total energy $E_{\rm tot}$ can be given by

$$E_{\rm tot} = E_{\rm ex} + E_{\rm PMA} + E_{\rm Ze} + E_{\rm demag} + E_{\rm DMI} + E_{\rm me}, \quad (1)$$

where $E_{\rm ex}$ is the nearest neighbor exchange coupling energy, $E_{\rm PMA}$ is the uniaxial magnetic anisotropy energy, $E_{\rm Ze}$ is the Zeeman energy, $E_{\rm demag}$ is the demagnetizing field energy, $E_{\rm DMI}$ is the DMI energy, and $E_{\rm me}$ is the magneto-elastic energy. The different topological magnetic structures of magnonic crystals based on domains or skyrmions can be formed through the competitions of these energies and the ground states can be obtained with the certain initial magnetic distributions.

Secondly, we studied the strain-manipulated dispersion characteristics of the magnonic crystals by solving the Landau–Lifshitz–Gilbert (LLG) equation which can be given by

$$\frac{\partial \boldsymbol{m}(r,t)}{\partial t} = -\mu_0\gamma(\boldsymbol{m}(r,t)\times \boldsymbol{H}_{\rm eff}) + \alpha\left(\boldsymbol{m}(r,t)\times\frac{\partial \boldsymbol{m}(r,t)}{\partial t}\right), \quad (2)$$

where $\boldsymbol{m}(r,t)$ is the unit magnetization vector, α is the dimensionless Gilbert damping coefficient, γ is the gyromagnetic ratio, μ_0 is the vacuum permeability, and $\boldsymbol{H}_{\rm eff}$ is the effective magnetic field which can be introduced by calculating the differential of $E_{\rm tot}$ to $\boldsymbol{m}(r,t)$. After collecting the spin excitations among time and space, the dispersion relations can be obtained by performing the 2D double fast Fourier transform (2D-FFT). In addition, the strain-manipulated effects were considered by introducing the magneto-elastic energy which can be described as

$$E_{\rm me} = B_1\sum_{i=x,y,z} m_i^2\varepsilon_{ii} + B_2\sum_i\sum_{j\neq i} m_i m_i \varepsilon_{ij}. \quad (3)$$

Here, B_1 and B_2 are the magnetoelastic coupling constants which are related to magnetostriction constants and the elastic constants.[32] ε_{ij} is the strain tensor which is performed to describe the applied strain. In this work, biaxial in-plane strains are considered and the strain tensor can be reduced to

$$\varepsilon = \varepsilon_{xx} = \varepsilon_{yy} = -\varepsilon_{zz}, \quad \varepsilon_{ij,i\neq j} = 0. \quad (4)$$

In addition, the applied strain is compressive when $\varepsilon < 0$ and tensile when $\varepsilon > 0$.

In our simulations, Co nano-layers were used to hold the magnonic crystals with varied DMI strength. The typical material parameters for Co were taken as: saturation magnetization $M_{\rm s} = 5.8\times10^5$ A/m, exchange stiffness constant $A_{\rm ex} = 1.5\times10^{-11}$ J/m, Gilbert damping coefficient $\alpha = 0.005$, gyromagnetic ratio $\gamma = 2.211\times10^5$ m/(A·s), magneto-elastic coupling constants $B_1 = -1.617\times10^7$ N/m^2 and $B_2 = 2.31\times10^6$ N/m^2.[33–35] Here, setting a low Gilbert damping coefficient can improve the quality of the dispersion curves.[36–38] The magnonic crystal layer is 2000 nm×50 nm×1 nm and the simulated mesh cell is 2 nm×2 nm×1 nm.

3. Results and discussion

First of all, we studied the stability of strain-manipulated magnonic crystals with DMI. Figure 1(a) presents the simulated structure consisting of a piezoelectric substrate (PE), a heavy metal layer (HM), and a ferromagnetic (FM) ultrathin layer. With symmetry breaking at interface between HM layer and FM layer, DM interaction could be introduced in FM ultrathin layer. The voltage is applied to the PE layer in which the strain can be induced by converse piezoelectric effect, and for typical piezoelectric materials such as $LiNbO_3$ or PZT, strains ranging from −0.6% to 0.6% can be induced by voltages lower than 10 V.[39–41] With manipulating the DMI strength and strain strength, the magnetic layer can present several different topological magnetic distributions as shown in Fig. 1(b). Magnonic crystals with domain state can be achieved with periodically arranged magnetic domains with opposite magnetizations. We can also observe skyrmion state which presents periodically distributed skyrmions along the central line and zigzag state which presents periodically distributed half skyrmions along both side of the edges. Meanwhile, we can also observe irregular magnetic distributions which is indicated as maze state.

To understand the strain-manipulated and DMI-dependent stabilities of the magnonic crystals, we investigated the phase diagram with changing strain strength ε and DMI strength D. In our simulation, the stable distribution could be achieved by minimizing the total energy, so the competitions among energies with given initial magnetic distributions would determine the final stable state. Figures 2(a) and 2(b) present the phase diagrams with changing ε from −3.0% to

3.0% and changing D from 0.5 mJ/m^2 to 5 mJ/m^2. The perpendicular anisotropy constant K is set to be 8×10^5 J/m^3 and the static magnetic field H is set to be 1×10^4 A/m. In the simulation of Figs. 2(a) and 2(b), we chose the domain-like states and skyrmion-like states as the simulation initial states, respectively. The domain-like initial states are periodically arranged domain magnetizations with unit magnetization vector $m_z=+1$ or $m_z=-1$, while the skyrmion-like initial states present periodically arranged circularly magnetizations with $m_z=-1$ embedded in the uniformly magnetized layer with $m_z=+1$. We can see that the phase diagrams present obviously different stable state distributions for both of domain-like and skyrmion-like initial states.

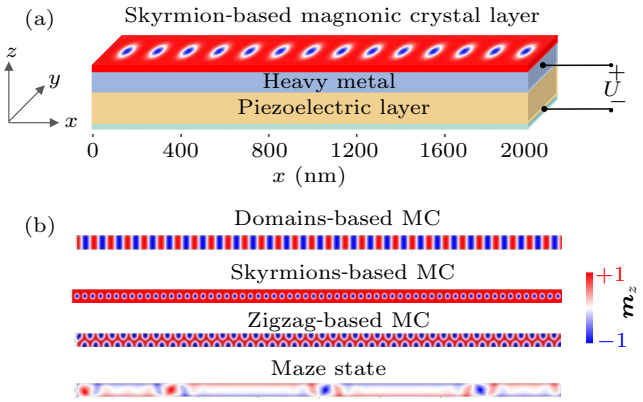


Fig. 1. (a) The schematic diagram of the proposed strain-manipulated magnonic crystal based on skyrmion. (b) Topological magnetic distributions for periodic domain-based magnonic crystal, skyrmion-based magnonic crystal, zigzag-based magnonic crystal, and non-periodic maze state.

As shown in Fig. 2(a), only two stable states are achieved in the range of varied ε and D values. Uniformly ferromagnetic state can be observed with increasing the compressive strain and decreasing the strength of DMI. At meantime, domain state can be observed with increasing both of the tensile strain and the DMI strength. Particularly, the domain states can present different period with manipulated ε and D. The period of each final stable state is labelled in Fig. 2(a) and we can see that, the period can be manipulated from 13 to 50. In addition, considering that the simulation step of ε and D is 0.6% and 0.5 mJ/m^2, respectively, it is suggested that much precise period values can be obtained with decreasing the simulation step of ε and D. However, we can see that, higher tensile strain and larger value of D are favor to stabilize the domain state.

Different to stable states with domain-like initial state, stable states with skyrmion-like initial state present several complex topological magnetic structures including ferromagnetic state, skyrmion state, domain state, zigzag state and maze state, as shown in Fig. 2(b). We can see that, ferromagnetic state or skyrmion state can be achieved under tensile strain with changing D values from 0.5 mJ/m^2 to 5.0 mJ/m^2. Moreover, lower tensile strain and larger DMI strength are favor to exhibit skyrmion state. At meantime, ferromagnetic or skymion state converts to domain state, zigzag state or maze state with decreasing the tensile strain and increasing the compressive strain. In particular, skyrmions-based magnonic crystals can only hold in very narrow ranges of applied strain which are indicated by stars as shown in Fig. 2(b).

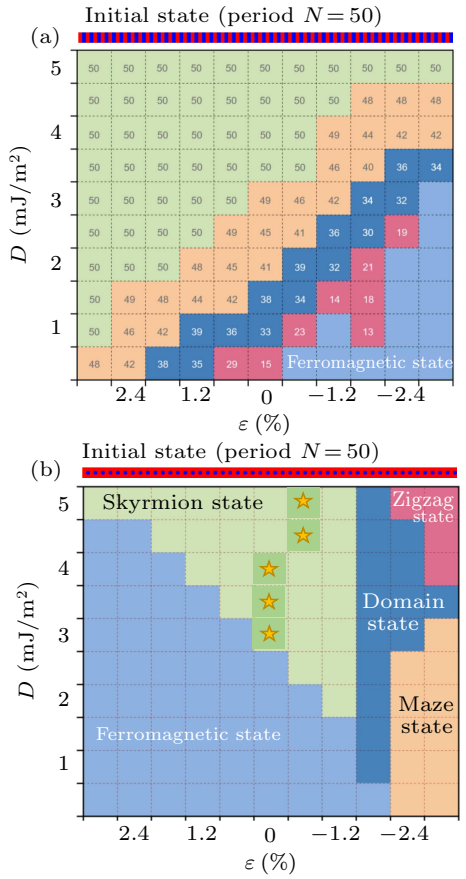


Fig. 2. Phase diagrams of strain strength ε versus DMI strength D with (a) domain-like initial state and (b) skyrmion-like initial state. ($K=8\times10^5$ J/m^3, $H=1\times10^4$ A/m).

As we all know, periodical magnetic distributions such as magnonic crystals based on domains or skyrmions can manipulate the propagation of the spin wave. Next, we continue to study strain-manipulated dispersion relations of magnonic crystals with DMI, especially magnonic crystals based on domains and skyrmions.

Firstly, we studied the strain-manipulated dispersion relations of domains-based magnonic crystals. Figure 3 presents the dispersion relations calculated in the domains-based magnonic crystals under different strains: $\varepsilon=-1.8\%$, $\varepsilon=0$, and $\varepsilon=1.8\%$, represented as the frequency versus wavenumber. The DMI constant D is set to be 3 mJ/m^2. In order to get the dispersion relations, a sine cardinal magnetic field was applied to the central area to excite spin waves in the magnonic crystals. The sine cardinal magnetic field can be described as

$$H_z'(t)=H_{z0}'\frac{\sin\left[\omega\left(t-t_0\right)\right]}{\omega\left(t-t_0\right)} \tag{5}$$

with cutoff frequency $f = 100$ GHz and amplitude $H'_{z0} = 100$ A/m. Then the fluctuations of magnetization ($\delta m_z(x,t) = m_z(x,t) - m_z(x,0)$) were collected during 10 ns along the line from (0 nm, 50 nm, 1 nm) to (2000 nm, 50 nm, 1 nm). After that, the 2D-FFT was executed to the evolution of $\delta m_z(x,t)$ to obtain the frequency–wavenumber relations which represents the dispersion characteristics of the propagating spin waves. It should be noticed that, the skyrmion also can be moved by the propagating spin waves.[12–18] In our simulation, the amplitude of the exciting magnetic field is 1% of the static magnetic field, and the sine cardinal magnetic field with cutoff frequency of 100 GHz can be treated as the superposition of sin-function magnetic fields with frequencies ranging from 0 GHz to 100 GHz, which can be considered as perturbations.[36]

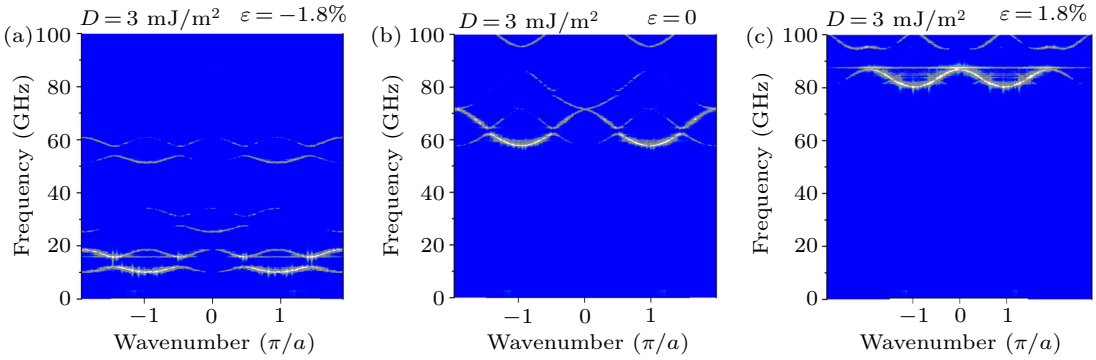


Fig. 3. Dispersion relations of the domains-based magnonic crystals with strain (a) $\varepsilon = -1.8\%$, (b) $\varepsilon = 0\%$, and (c) $\varepsilon = 1.8\%$. $K = 8 \times 10^5$ J/m^3, $H = 1 \times 10^4$ A/m.

As shown in Fig. 3, the dispersion relations under three different strains all present periodic characteristics with folded branches. These branches or allowed bands indicate that the spin waves can propagate through the magnonic crystals at definite wavenumbers and frequencies. At meantime, the spin waves with some other frequencies ranging in the bandgaps cannot propagate through the magnonic crystals. The obtained dispersion characteristics in magnonic crystals are similar to those in condensed solid crystals and photonic crystals, which indicates the propagations of electrons and photons. Furthermore, the strain-manipulated dispersion relations were investigated. As shown in Fig. 3, the dispersion branches shift to higher frequencies with strain changing from compressive ($\varepsilon = -1.8\%$) to tensile ($\varepsilon = 1.8\%$). Particularly, the widths of the allowed bands and the forbidden bands are changing with the strains. In addition, it can be seen that, the energy branches exhibit weakening intensities with increasing the frequency, which is due to the numerical simulation configurations, such as simulation times, simulation steps or cell discretizations.

In order to investigate the strain-manipulated dispersion characteristics clearly, we summarized the strain dependencies of the four lower allowed bands and the forbidden bands for domains-based magnonic crystals with $D = 3$ mJ/m^2, 4 mJ/m^2, and 5 mJ/m^2, as shown in Fig. 4. The simulated value of strain ε changes from -3.0% to 3.0% and the periodic domains-based magnonic crystals can be achieved in the range of ε changing from -1.8% to 2.7% for $D = 3$ mJ/m^2, from -2.1% to 3.0% for $D = 4$ mJ/m^2, and from -2.1% to 3.0% for $D = 5$ mJ/m^2, as denoted by 'II' in Figs. 4(a)–4(c). No magnonic crystals based on topological magnetic structure is obtained with ε changing in the range denoted by 'I' and 'III'.

As shown in Fig. 4(a), the four lower allowed bands are lifted to higher frequency range when the compressive strain is decreased. In addition, the bandwidths of the four lower allowed bands keep increasing with the compressive strain decreased to zero. Moreover, these observed allowed bands are lifted to higher frequency range when the tensile strain is increased from 0% to 1.8% and then dropped to lower frequency range when the tensile strain is increased from 1.8% to 2.7%. At meantime, the allowed band 1 and 2 merge to an identical band, while the allowed band 3 and 4 merge to another identical band.

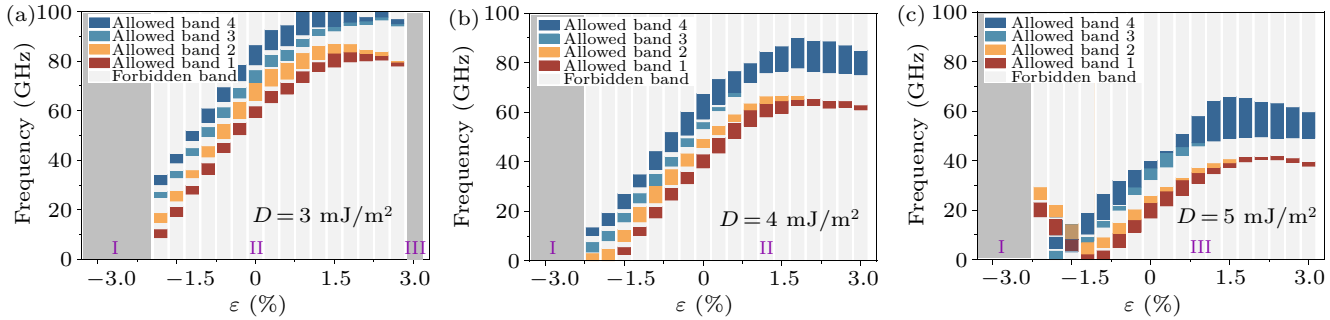


Fig. 4. Strain dependencies of the allowed bands and forbidden bands for domains-based magnonic crystals with (a) $D = 3$ mJ/m^2, (b) $D = 4$ mJ/m^2, and (c) $D = 5$ mJ/m^2. $K = 8 \times 10^5$ J/m^3, $H = 1 \times 10^4$ A/m.

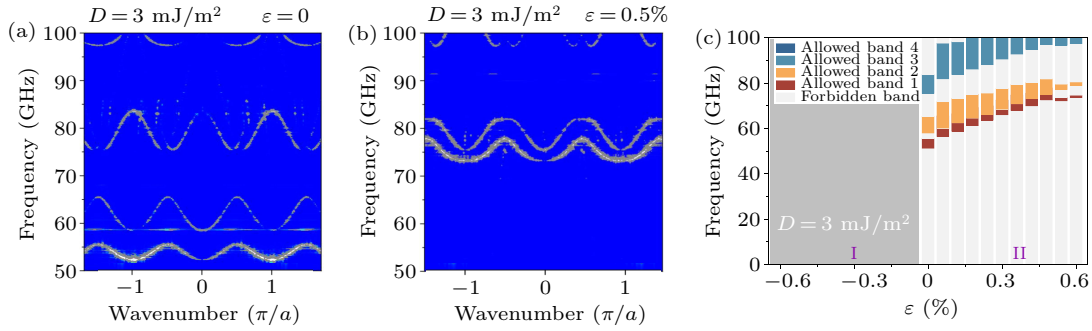


Fig. 5. Dispersion relations of the skyrmions-based magnonic crystals with strain (a) $\varepsilon = 0\%$ and (b) $\varepsilon = 0.5\%$. (c) Strain dependencies of the allowed bands and forbidden bands. $D = 3$ mJ/m^2, $K = 8 \times 10^5$ J/m^3, $H = 1 \times 10^4$ A/m.

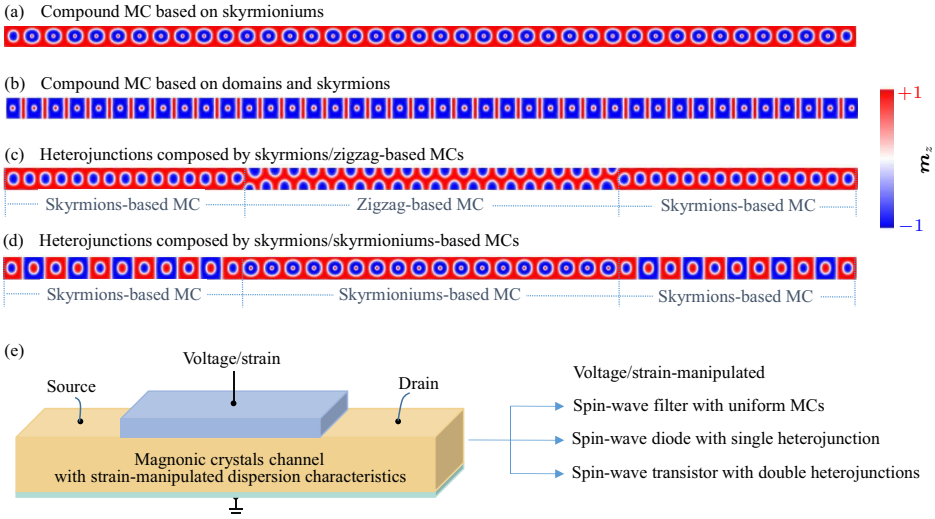


Fig. 6. Compound magnonic crystals based on (a) periodically arranged skyrmioniums ($D = 5$ mJ/m^2, $K = 0.8 \times 10^5$ J/m^3, $H = 1 \times 10^4$ A/m, $\varepsilon = 0$) and (b) periodically arranged domains and skyrmions ($D = 5$ mJ/m^2, $K = 1 \times 10^5$ J/m^3, $H = -8 \times 10^5$ A/m, $\varepsilon = -0.56\%$). Magnonic crystal heterojunctions composed by (c) skyrmions-based magnonic crystal and zigzag-based magnonic crystal ($D = 5$ mJ/m^2, $K = 7 \times 10^5$ J/m^3, $H = 1 \times 10^4$ A/m, $\varepsilon = 0.25\%$) and (d) skrymions-based magnonic crystal and skyrmioniums-based magnonic crystal ($D = 5$ mJ/m^2, $K = 8 \times 10^5$ J/m^3, $H = 1 \times 10^4$ A/m, $\varepsilon = 0.21\%$). (e) Proposed voltage/strain-manipulated spin-wave devices based on magnonic crystals with DMI.

As shown in Fig. 4(b), similar strain-manipulated variation trends of the discussed allowed bands are achieved in domains-based magnonic crystals for $D = 4$ mJ/m^2, which is that the bands are lifted firstly and then dropped with applied strain changing from compressive -2.1% to tensile 3.0%, and also, the four allowed bands merge to two identical bands. Comparing with the strain-manipulated dispersion characteristics achieved for $D = 3$ mJ/m^2 and $D = 4$ mJ/m^2, the dispersion relations present different behaviors for $D = 5$ mJ/m^2. As shown in Fig. 4(c), the allowed bands 1 and 2 are dropped to lower frequency range when the compressive strain is increased to -1.8% and then are annihilated when the compressive strain is -2.1%. Particularly, the allowed bands 3 and 4 are dropped to lower frequency range when the compressive strain is increased to -1.2% and then lifted to higher frequency range when the compressive strain is increased from -1.2% to -2.1%. Similarly, two merged allowed bands are achieved with high tensile strain. Furthermore, for $D = 3$ mJ/m^2 as presented in Fig. 4(a), the frequency in the middle of the allowed band 1 changes from minimum value of 10.4 GHz to maximum value of 81.5 GHz with varied applied strains, the variation of which is as high as 71.1 GHz, while the varied value of allowed band 3 is also as high as 70.9 GHz, which demonstrate that the change of spin-wave frequency by strains is very large, and indicate remarkable manipulation effects.

Secondly, we studied the strain-manipulated dispersion characteristics of skyrmions-based magnonic crystals. The dispersion relations achieved in the skyrmions-based magnonic crystals without applied tensile strain and with strain $\varepsilon = 0.5\%$ are simulated and presented in Figs. 5(a) and 5(b), respectively. The summarized strain dependencies of the four lower allowed bands and the forbidden bands are shown in Fig. 5(c). It can be seen that, several distinct allowed frequency bands and forbidden frequency bands are observed, and the strain can manipulate the band widths and the positions. The denoted areas 'II' in Fig. 5(c) indicate the formations of skyrmions-based magnonic crystals with certain range of applied strains. We can see that, the widths of allowed bands 2 and 3 increase obviously when the tensile strain is 0.06% comparing with that when no strain is applied. Then, the widths of allowed bands 1 and 2 keep decreasing with increasing strain from 0.06% to 0.6%. At meantime, the band gap between allowed bands 2 and 3 keeps increasing with the

increased tensile strain. In addition, the allowed bands shift to higher frequencies with increasing the tensile strain from 0% to 0.48%, and then shift to a little lower frequency at $\varepsilon = 0.54\%$.

The above result has demonstrated that magnonic crystals based on domains or skyrmions can be obtained and the dispersion characteristics can be manipulated by applied strains. Akin to semiconductor solid crystals that the periodically arranged unit elements can be not only one kind of atoms but also several kinds of compound atoms, magnonic crystals can also be realized based on compound elements such as skyrmioniums (as shown in Fig. 6(a)) or domains and skyrmions (as shown in Fig. 6(b)). With more complex magnetic unit elements considered, the strain-manipulated dispersion characteristics would be more abundant and meaningful.

Furthermore, as key components in advanced spin-wave devices, heterojunctions can be realized in strain-manipulated magnonic crystals. With applied strains and other parameters finely tuned, part of the skyrmions-based magnonic crystals can converse to zigzag-based magnonic crystals as shown in Fig. 6(c) or skyrmioniums-based manonic crystals as shown in Fig. 6(d), which lead to two heterojunctions. In addition, the periods and the lengths of each magnonic crystal can be manipulated by applied strains. Above all, voltage or strain-manipulated spin-wave devices such as filters, diodes, and transistors, as shown in Fig. 6(e), can be realized based on this platform.

4. Conclusion

In summary, we theoretically investigated the strain-manipulated dispersion characteristics of magnonic crystals with DMI and proposed the potential applications in spin-wave devices. We started with investigating the ground states of the magnonic crystals. Then, the strain-manipulated dispersion characteristics of the magnonic crystals based on domains and skyrmions were studied. It is found that, the applied strain can manipulate the band widths and the positions of the allowed frequency bands. Particularly, the simulation results show that manipulation effect is remarkable and the frequency ranges of the allowed bands are very large, which still need further analytical explanations and experimental confirmation. At meantime, larger strains will also distort the periodic arrangement of the magnetic distributions, which should be considered in the characteristics of topological robustness.[42] Finally, we proposed the realization of magnonic crystal heterojunctions and potential applications in spin-wave devices such as filters, diodes, and transistors based on strain-manipulated magnonic crystals. The results may provide an interesting and effective platform for designing tunable spin-wave devices based on strain-manipulated magnonic crystals with DMI.

References

[1] Chumak A V, Sergra A A and Hillebrands B 2014 *Nat. Commun.* **5** 4700
[2] Vogt K, Fradin F, Pearson J, Sebastian T, Bader S, Hillebrands B, Hoffmann A and Schultheiss H 2014 *Nat. Commun.* **5** 3727
[3] Lee K S, Han D S and Kim S K 2009 *Phys. Rev. Lett.* **102** 127202
[4] Chumak A V, Vasyuchka V I, Sergra A A and Hillebrands B 2015 *Nat. Phys.* **11** 453
[5] Ma F, Zhou Y, Braun H B and Lew W S 2015 *Nano Lett.* **15** 4029
[6] Wang X G, Guo G H, Li Z X, Wang D W, Nie Y Z and Tang W 2015 *Europhys. Lett.* **109** 37008
[7] Li Z X, Wang X G, Wang D W, Nie Y Z, Tang W and Guo G H 2015 *J. Magn. Magn. Mater.* **388** 10
[8] Mruczkiewicz M, Gruszecki P, Zelent M and Krawczyk M 2016 *Phys. Rev. B* **93** 174429
[9] Wang X G, Nie Y Z, Xia Q L and Guo G H 2020 *J. Appl. Phys.* **128** 063901
[10] Dzyaloshinsky I 1958 *J. Phys. Chem. Solids* **4** 241
[11] Moriya T 1960 *Phys. Rev. Lett.* **4** 228
[12] Yang X X, Ai X L, Liu X, Li H T, Ma X P, Shim J H and Piao H G 2024 *Appl. Phys. Lett.* **125** 172403
[13] Abdulrazak T, Liu X J, Wang Z Y, Cao Y S and Yan P 2024 *Chin. Phys. B* **33** 107504
[14] Li N, Fan M M, Zeng X Y and Yan M 2024 *Symmetry* **16** 1336
[15] Saini S, Bindal N, Raj R K and Kaushik B K 2024 *Nanoscale* **16** 9004
[16] Bai X, Wang J N, Yang J X, Liu H B, Zhang S F and Liu Q F 2024 *J. Magn. Magn. Mater.* **15** 171231
[17] Ma X P, Ai X L, Yang X X, Cai M X, Shim J H and Piao H G 2023 *J. Magn. Magn. Mater.* **581** 170665
[18] Liu Y, Liu T T, Jin Z, Hou Z P, Chen D Y, Fan Z, Zeng M, Lu X B, Gao X S, Qin M H and Liu J M 2024 *Phys. Rev. B* **106** 064424
[19] Liu A K and Finkelstein A M 2023 *Phys. Rev. B* **107** 012413
[20] Grachev A A, Sheshukova S E and Sadovnikov A V 2024 *Appl. Phys. Lett.* **124** 162406
[21] Medlej I, Wang J L, Hu C Y and Yu K L 2024 *J. Magn. Magn. Mater.* **591** 171726
[22] Yang W G and Schmidt H 2021 *Appl. Phys. Rev.* **8** 021304
[23] Bandyopadhyay S, Atulasimha J and Barman A 2021 *Appl. Phys. Rev.* **8** 041323
[24] Zhu M M, Hu H M, Cui S T, Li Y T, Zhou X P, Qiu Y, Guo R D, Wu G H, Yu G L and Zhou H M 2021 *Appl. Phys. Lett.* **118** 262412
[25] Zhu M M, Li Y T, Hu H M, Cui S T, Qiu Y, Yu G L and Zhou H M 2022 *Appl. Phys. Lett.* **121** 032402
[26] Hu J M, Yang T N and Chen L Q 2020 *Acta Mater.* **183** 145
[27] Rendell-Bhatti F, Lamb R J, Jagt J W, Paterson G W, Swagten H J M and McGrouther D 2020 *Nat. Commun.* **11** 3536
[28] Dong S Z, Wang J, Shi X M, Liang D S, Mehdi Jafri H, Hu C C, Jin K and Huang H B 2023 *Scr. Mater.* **222** 114994
[29] Jin Z N, He X L, Yu C, Fang H N, Chen L and Tao Z K 2024 *Chin. Phys. B* **33** 017501
[30] Beg M, Lang M and Fangohr H 2022 *IEEE Trans. Mag.* **58** 7300205
[31] Fangohr H, Lang M, Holt S J R, Pathak S A, Zulfiqar K and Beg M 2024 *AIP Adv.* **14** 015138
[32] Hu J M, Yang T and Chen L Q 2020 *Acta Mater.* **183** 145
[33] Ota S, Hibino Y, Bang D, Awano H, Kozeki T, Akamine H, Fujii T, Namazu T, Takenobu T, Koyama T and Chiba D 2016 *Appl. Phys. Express* **9** 043004
[34] Biswas A K, Ahmad H, Atulasimha J and Bandyopadhyay S 2017 *Nano Lett.* **17** 3478
[35] Zhu M, Li Y, Hu H, Cui S, Qiu Y, Yu G and Zhou H 2022 *Appl. Phys. Lett.* **121** 032402
[36] Venkat G, Kumar D, Franchin M, Dmytriiev O, Mruczkiewicz M, Fangohr H, Barman A, Krawczyk M and Prabhakar A 2013 *IEEE Trans. Magn.* **49** 524
[37] Schoen M A W, Thonig D, Schneider M L, Silva T J, Nembach H T, Eriksson O, Karis O and Shaw J M 2016 *Nat. Phys.* **12** 839
[38] Barati E, Cinal M, Edwards D M and Umerski A 2014 *Phys. Rev. B* **90** 0014420
[39] https://unitedcrystals.com/LiNbO3Prop.html
[40] Yokouchi Y, Sugimoto S, Rana B, Seki S, Ogawa N, Kasai S and Otani Y 2020 *Nat. Nanotechnol.* **15** 361
[41] https://info.piezo.com/hubfs/data-sheet
[42] Rosales H Diego and Troncoso E Roberto 2024 *Phys. Rev. B* **110** 134435